Molecular Cell
Article

Active and Repressive Chromatin Are Interspersed without Spreading in an Imprinted Gene Cluster in the Mammalian Genome

Kakkad Regha,[1,4] Mathew A. Sloane,[1,4] Ru Huang,[1] Florian M. Pauler,[1] Katarzyna E. Warczok,[1] Balázs Melikant,[2,5] Martin Radolf,[3] Joost H.A. Martens,[3,6] Gunnar Schotta,[3] Thomas Jenuwein,[3] and Denise P. Barlow[1,*]

[1] CeMM Research Center for Molecular Medicine of the Austrian Academy of Sciences, Institute of Genetics, Max F. Perutz Laboratories, Vienna Biocenter, Dr. Bohr-Gasse 9/4, A-1030 Vienna, Austria
[2] Institute of Genetics, Max F. Perutz Laboratories, Vienna Biocenter, Dr. Bohr-Gasse 9/4, A-1030 Vienna, Austria
[3] Research Institute of Molecular Pathology, Dr. Bohr-Gasse 7, A-1030 Vienna, Austria
[4] These authors contributed equally to this work.
[5] Present address: Intercell AG, Campus Vienna Biocenter 2, A-1030 Vienna, Austria.
[6] Present address: NCMLS #191, Molecular Biology, P.O. Box 9101, 6500 HB Nijmegen, The Netherlands.
*Correspondence: denise.barlow@univie.ac.at
DOI 10.1016/j.molcel.2007.06.024

SUMMARY

The *Igf2r* imprinted cluster is an epigenetic silencing model in which expression of a ncRNA silences multiple genes in *cis*. Here, we map a 250 kb region in mouse embryonic fibroblast cells to show that histone modifications associated with expressed and silent genes are mutually exclusive and localized to discrete regions. Expressed genes were modified at promoter regions by H3K4me3 + H3K4me2 + H3K9Ac and on putative regulatory elements flanking active promoters by H3K4me2 + H3K9Ac. Silent genes showed two types of nonoverlapping profile. One type spread over large domains of tissue-specific silent genes and contained H3K27me3 alone. A second type formed localized foci on silent imprinted gene promoters and a nonexpressed pseudogene and contained H3K9me3 + H4K20me3 ± HP1. Thus, mammalian chromosome arms contain active chromatin interspersed with repressive chromatin resembling the type of heterochromatin previously considered a feature of centromeres, telomeres, and the inactive X chromosome.

INTRODUCTION

Genomic imprinting is a *cis*-acting epigenetic mechanism that results in identical gene sequences being treated differently by the transcription machinery simply because of their inheritance from a maternal or paternal parent. Imprinted expression is restricted to a few hundred genes in the mammalian genome, most of which are found in small clusters. Imprinting of a gene cluster is regulated by an imprint control element that is inactivated on one parental chromosome by a DNA methylation imprint (Solter, 2006). The majority of the genes in an imprinted cluster are mRNA genes; however, at least one is always a noncoding RNA (ncRNA). The function of the ncRNA has been tested in three imprinted clusters. In the *Igf2* cluster, the *H19* ncRNA has no direct silencing role; instead, silencing operates via an insulator mechanism (Lewis and Reik, 2006). However, in the *Igf2r* and *Kcnq1* imprinted clusters, the *Air* and *Kcnq1ot1* ncRNAs have both been shown to play a direct silencing role (Mancini-Dinardo et al., 2006; Sleutels et al., 2002).

In the two imprinted clusters with functional ncRNAs, one chromosome expresses the ncRNA and silences flanking clustered mRNA genes, while the other chromosome shows the reciprocal expression pattern. Moreover, in these two cases the expressed ncRNA promoter is located in an intron of one of the silenced genes in the cluster. This type of expression pattern, in which closely spaced genes are silent or expressed, indicates that repressive chromatin would not spread throughout an imprinted cluster. Historically, chromatin has been classified by its appearance in interphase nuclei stained with basic dyes as either heterochromatin or euchromatin, which are considered to represent, respectively, the repressed and active regions of the genome (Huisinga et al., 2006). In mammals, heterochromatin-associated histone modifications have only been characterized at pericentric and telomeric regions and the inactive X chromosome (Chadwick and Willard, 2004; Garcia-Cao et al., 2004; Schotta et al., 2004). This has identified H3K9me3, H4K20me3, H3K27me1, and HP1 proteins as markers of pericentric and telomeric regions and two distinct nonoverlapping patterns comprising either H3K9me3 + H4K20me3 + HP1 or *Xist* ncRNA + macroH2A + H3K27me3 on the inactive X chromosome. It is not yet known if short genomic regions containing silent genes that lack visible staining by basic

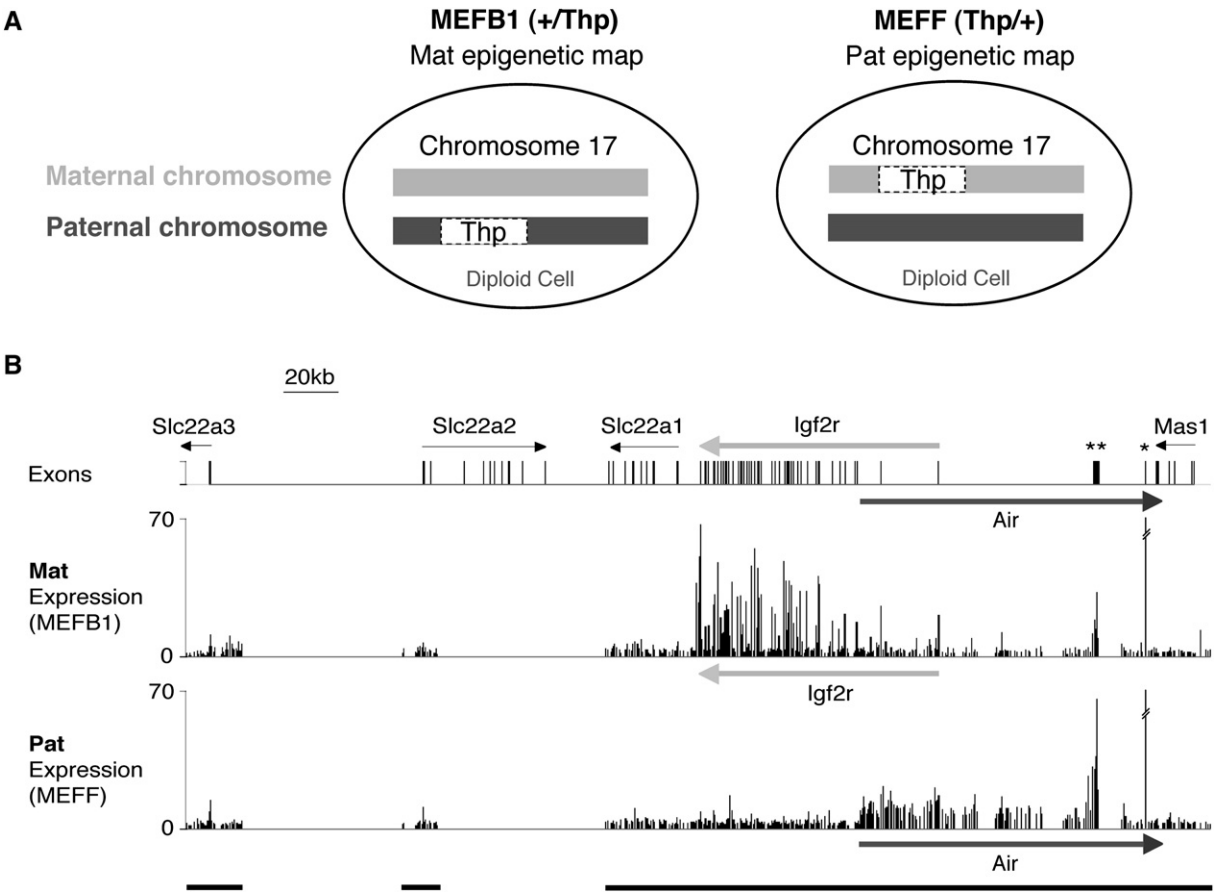

Figure 1. Expression Profile of the *Igf2r* Imprinted Cluster

(A) Mouse embryo fibroblast cells (MEFB1 and MEFF) used to detect parental-specific expression and epigenetic modifications were prepared from 13.5 dpc +/Thp and Thp/+ embryos. +, wild-type chromosome 17. T^{hp}, T hairpin chromosome 17 variant contains a 6 Mbp deletion including the 500 kb *Igf2r* imprinted cluster. The maternal chromosome is written on the left side.

(B) Top row, 380 kb map showing the *Slc22a3*, *Slc22a2*, *Slc22a1*, *Igf2r*, and *Mas1* genes. The *Air* promoter lies in *Igf2r* intron 2. *Air* is a 108 kb single-exon ncRNA that overlaps *Igf2r* and *Mas1* in antisense orientation. Bars, exons or pseudogenes. Thin arrows, silent genes in MEF cells. Thick arrows, maternally expressed gene (light gray), paternally expressed gene (dark gray). **L41* pseudogene, ***Au76* pseudogene. The Mat Expression (MEFB1) and Pat Expression (MEFF) rows show cDNA hybridization to a custom PCR tiling array spanning three regions: 19 kb containing the *Slc22a3* promoter, 13 kb containing the *Slc22a2* promoter, and 220 kb from *Slc22a1*-3′ end to *Mas1*-3′ end (indicated by black bars underneath). Each column is the mean ratio of medians of eight replicate spots.

dyes can also be defined as heterochromatin or if they represent another form of repressed chromatin. Imprinted clusters represent an ideal model system to investigate this, as known imprinted clusters are located in short domains spanning 100–3000 kb and, in addition to imprinted genes, are interspersed with genes that show biparental expression or tissue-specific silencing (http://www.mgu.har.mrc.ac.uk/research/imprinting/imprin-intro.html).

The mouse *Igf2r* imprinted gene cluster spans 500 kb (Figure 1) and contains the paternally expressed *Air* ncRNA and the maternally expressed *Igf2r* mRNA that show widespread imprinted expression in fetal, placental, and adult tissue, plus the maternally expressed *Slc22a2* and *Slc22a3* mRNAs that are not expressed in fetal tissue but show imprinted expression in placenta (Regha et al., 2006). The *Air* promoter is located in *Igf2r* intron 2 and generates an antisense transcript across the 5′ part of the *Igf2r* gene. Expression of the *Air* ncRNA has been shown to silence *Igf2r*, *Slc22a2*, and *Slc22a3* on the paternal chromosome (Sleutels et al., 2002). Surprisingly, however, transcriptional overlap between *Air* and *Igf2r* is not necessary for silencing flanking genes in the cluster (Sleutels et al., 2003). A second type of silencing is present on the maternal chromosome, which lacks *Air* expression because the *Air* promoter is directly repressed by a DNA methylation imprint acquired during female gametogenesis (Seidl et al., 2006). A methylation imprint acquired in late development that is a consequence, not a cause, of silencing is also found on the silenced paternal *Igf2r* promoter. However, widespread differential DNA methylation does not mark the three genes silenced by the *Air* ncRNA (Stoger et al., 1993; Zwart et al., 2001). Allele-specific

histone lysine methylation marks have also been identified on the silent and active *Air* and *Igf2r* promoters; however, their distribution throughout the region is not known (Fournier et al., 2002; Vu et al., 2004).

We use here chromatin immunoprecipitation (ChIP) interrogated by PCR or genome tiling arrays (ChIP-Chip) to map the chromatin profile of the *Igf2r* cluster in mouse embryonic fibroblast (MEF) cells. Surprisingly, silencing of the paternal *Igf2r* promoter by the *Air* ncRNA, and silencing of the maternal *Air* promoter by DNA methylation, does not involve spreading of repressive chromatin. Instead, we show that these silent imprinted promoters and a nonexpressed pseudogene are marked by focal repressive histone modifications resembling those identified at centromeres and telomeres. Furthermore, as these heterochromatic foci are embedded inside active transcription units, they do not block transcription elongation. In contrast, a cluster of flanking tissue-specific silenced genes was modified by a broad domain marked by one type of repressive histone modification. These data show that mammalian chromosome arms contain discrete regions of different types of repressive chromatin previously considered a feature of centromeres, telomeres, and the inactive X chromosome.

RESULTS

Expression Profile of the *Igf2r* Imprinted Cluster in T^{hp} MEF Cells

We used here MEF cells carrying either a paternal (MEFB1, $+/T^{hp}$) or maternal (MEFF, $T^{hp}/+$) T^{hp} deletion, which includes the 500 kb *Igf2r* imprinted cluster (Figure 1A). Expression of genes in this region in MEFs was determined by cDNA hybridization to a custom PCR tiling array. Figure 1B shows that only *Igf2r* is expressed from the maternal allele (middle line) and only *Air* from the paternal allele (bottom line). *Igf2r* signals correspond to the 48 gene exons while *Air* ncRNA signals were detected on all PCR fragments throughout the length of unspliced 108 kb *Air* transcript. Note that the *Air* promoter lies in *Igf2r* intron 2, and thus on both parental chromosomes a silent promoter is overlapped by an expressed transcript. Expression of the remaining four tissue-specific silenced genes in this region (*Slc22a3*, *Slc22a2*, *Slc22a1*, and *Mas1*) was not detected from either chromosome in MEF cells. Hybridization signals were detected on both parental chromosomes at the *Au76* and *L41* pseudogenes (psg) contained within the *Air* gene body that represent crosshybridization from expressed genomic copies (Figure 1B, see Figure S1 in the Supplemental Data available with this article online). In MEFB1 and MEFF cells, the DNA methylation status of the *Igf2r*, *Air*, *Slc22a2*, and *Slc22a3* promoters was as previously described (Zwart et al., 2001), and *Au76*-psg was equally methylated on both parental alleles (Figure S1, Table S3).

These MEF cells represent a homogenous population of differentiated cells that allows examination of parental-specific chromatin profiles of three categories of silenced genes: (1) DNA methylation silencing of the maternal *Air* promoter (Seidl et al., 2006), (2) *Air* ncRNA silencing of the paternal *Igf2r* promoter (Sleutels et al., 2002), and (3) tissue-specific biparental silencing of the flanking *Slc22a1*, *a2*, *and a3* genes (Zwart et al., 2001).

Chromatin Modifications at the Maternal *Air* Promoter Silenced by DNA Methylation

ChIP-PCR was used to test the expressed *Igf2r* and silent *Air* promoter regions on the maternal chromosome for active (Figures 2C–2E) and repressive (Figures 2F–2J) histone modifications. Immunoprecipitated ChIP and Input DNA were used as templates for PCR with 24 primer pairs spanning 12 kb around the *Air* and *Igf2r* transcription starts at approximately 1 kb intervals. Note that the silent *Air* promoter is overlapped by transcription from the expressed *Igf2r* promoter 28 kb away and that four DNaseI hypersensitive (DHS) sites lie in these two regions, of which only DHSXII is maternal specific (Pauler et al., 2005).

Figures 2C–2E (right panels) show that the expressed *Igf2r* promoter region is enriched for H3K4me3, H3K4me2, and H3K9Ac. The downstream silent *Air* promoter region (left panels) was generally depleted for these modifications except for primer pairs 1–4 linked to DHSVII and VIII. On the expressed *Igf2r* promoter, H3K4me3 showed a focal distribution being most strongly enriched on primers that flank the transcription start. H3K4me2 showed a broader asymmetric distribution being enriched over the transcription start and in the direction of *Igf2r* transcription. H3K9Ac modifications resembled those of H3K4me2. ChIP-PCR using antibodies to multiple acetylation sites confirmed depletion of H3K9 and H3K14 acetylation on the silent *Air* promoter and enrichment on DHS sites. However, abundant H4 (K5 + K8 + K12 + K16) acetylation was detected throughout the silent *Air* and expressed *Igf2r* promoter regions (Figure S2).

Figures 2F and 2G (left panels) show strong H3K9me3 and H4K20 me3 (spanning 4–6 kb) at the silent *Air* promoter that were absent from the expressed *Igf2r* promoter (right panels). H4K20me1 and H3K27me1 were generally present throughout the silent *Air* promoter region and also found downstream, but not upstream of the expressed *Igf2r* transcription start (Figures 2H and 2J). H3K27me3 (Figure 2I), H3K27me2, H4K20me2, H3K9me1, and K3K9me2 (Figure S3) were absent from both the silent *Air* and the expressed *Igf2r* promoter regions. These data show the *Air* promoter (silenced by DNA methylation) and the expressed *Igf2r* promoter and are marked by focal repressive and active histone modifications that show limited spreading.

Chromatin Modifications at the Paternal *Igf2r* Promoter Silenced by the *Air* ncRNA

Figures 2K–2T show a parallel analysis of *Air* ncRNA-mediated silencing of the *Igf2r* promoter, which shows a similar pattern of focal modifications. On the paternal chromosome, the expressed *Air* promoter (left panel, Figures 2M–2O) is modified by focal H3K4me3, H3K4me2,

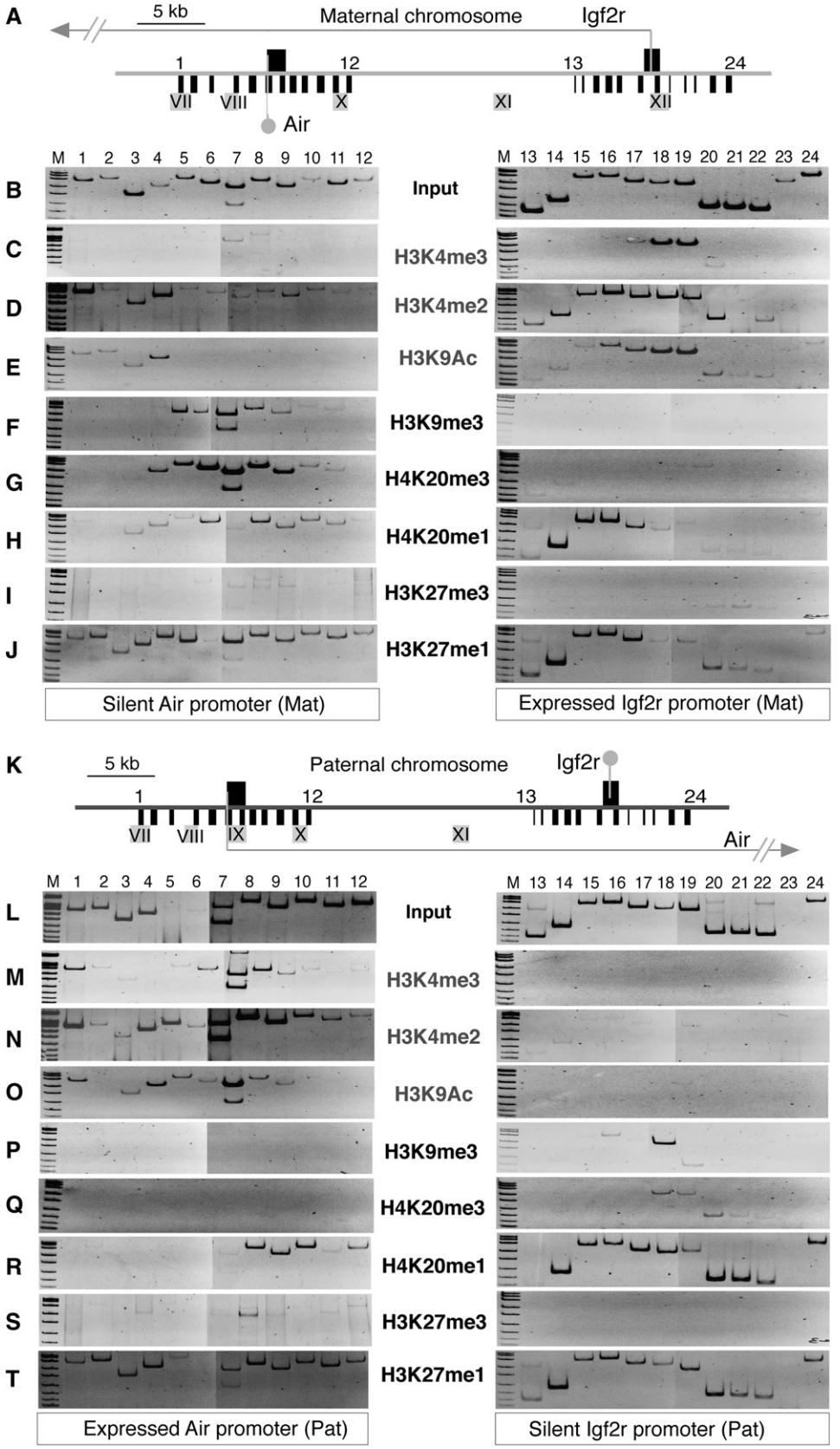
A
5 kb
Maternal chromosome
Igf2r
1
12
13
24
VII
VIII
X
XI
XII
Air
M 1 2 3 4 5 6 7 8 9 10 11 12
M 13 14 15 16 17 18 19 20 21 22 23 24
B
Input
C
H3K4me3
D
H3K4me2
E
H3K9Ac
F
H3K9me3
G
H4K20me3
H
H4K20me1
I
H3K27me3
J
H3K27me1
Silent Air promoter (Mat)
Expressed Igf2r promoter (Mat)
K
5 kb
Paternal chromosome
Igf2r
1
12
13
24
VII
VIII
IX
X
XI
Air
M 1 2 3 4 5 6 7 8 9 10 11 12
M 13 14 15 16 17 18 19 20 21 22 23 24
L
Input
M
H3K4me3
N
H3K4me2
O
H3K9Ac
P
H3K9me3
Q
H4K20me3
R
H4K20me1
S
H3K27me3
T
H3K27me1
Expressed Air promoter (Pat)
Silent Igf2r promoter (Pat)

and H3K9Ac, while the downstream silent *Igf2r* promoter (right panel) lacks these modifications. H3K4me2 modifications spread further in the direction of *Air* transcription but do not reach the silent *Igf2r* promoter. H3K9Ac was specific to the expressed *Air* promoter region; however, antibodies to multiple acetylation sites showed more widespread distribution of H3 and H4 acetylation throughout both silent and expressed promoter regions on the paternal chromosome (Figure S2). The modifications on nonpromoter DHS on the paternal chromosome were similar to that described above for the maternal chromosome. DHSX was modified by H3K4me2 alone, and DHSVII and VIII (primer pairs 1–4) were modified by H3K4me2 + H3K9Ac. DHSVII was additionally modified on the paternal chromosome by H3K4me3 (Figure 2M, primer pair 1). All DHS lacked specific repressive modifications, but some were covered by H4K20me1 and H3K27me1 (Figures 2R and 2T).

Figures 2P and 2Q show that H3K9me3 and H4K20me3 modifications were present on the silent *Igf2r* promoter, albeit to a lesser extent than at the silent *Air* promoter, but were absent from the expressed *Air* promoter. Similar to the maternal chromosome, H4K20me1 and H3K27me1 were found at both active and silent promoters (Figures 2R and 2T); however, only H4K20me1 was depleted upstream of the active *Air* promoter on the paternal chromosome. H3K27me3 (Figure 2S), H3K27me2, H4K20me2, H3K9me1, and H3K9me2 (Figure S3) were absent from both the expressed *Air* and silent *Igf2r* promoter regions on the paternal chromosome.

Quantitative PCR of H3K4me3, H3K4me2, and H3K9me3 modifications at the active and silent *Air* promoters supports the interpretation that expressed and silent promoters show mutually exclusive active and repressive histone modifications (Table S1). The enrichment of the expressed/silent *Air* promoter at primer pairs 1, 4, 5/6, and 6 is, respectively, 5.4, 0.8, 11.3, 234.2 (for H3K4me3), and 3.0, 54.5, 59.7, and 330.8 (for H3K4me2 for primer pairs 4, 5/6, 6, and 7). H3K9me3 at primer pairs 5/6 and 6 shows, respectively, 11.8- and 17.5-fold enrichment of the silent/expressed *Air* promoters.

Focal Active and Repressive Histone Modifications Intersperse without Spreading

It is notable from the ChIP-PCR of 12 kb at the *Air* and *Igf2r* promoter regions that the tested histone modifications do not spread through the body of the expressed or silent gene. To further examine the distribution of active and repressive histone modifications within the *Igf2r* cluster, we performed ChIP-Chip using the same ChIP/Input samples analyzed in Figures 2 and 3 and the 250 kb custom PCR tiling array shown in Figure 1B. Figure 3 and Figure S4 show a ChIP-Chip analysis of three active (H3K4me3, H3K4me2, and H3K9Ac) and four repressive (H3K9me3, H4K20me3, H4K20me1, and HP1γ) modifications on the maternal chromosome in which *Air* is silenced by DNA methylation. H3K4me3 was detectable as a single peak at the expressed *Igf2r* promoter but was absent from the remainder of the tiling array that included silent CpG island promoters (e.g., *Slc22a3*) and silent CG poor promoters (e.g., *Slc22a2*, *Slc22a1*). H3K4me2 showed a broader peak at the expressed *Igf2r* promoter and was also absent from the four silent promoters on the tiling array. H3K4me2 modifications did not show widespread spreading but were found outside promoter regions including a large domain in *Igf2r* intron 1. H3K9Ac was detected with a profile broadly similar to H3K4me2. ChIP-Chip with antibodies recognizing multiple acetylation sites (H3K9+K14 or H4K5+K8+K12+K16) confirmed the general pattern for H3 acetylation, but H4 acetylation was more widespread on silent and expressed genes (Figure S5). ChIP-Chip also showed that H3K9me3, H4K20me3, and HP1γ were all localized to the silent *Air* promoter but were absent from promoters of the four tissue-specific silent genes in the cluster. H4K20me1, in contrast, was generally present throughout the 250 kb tiling array on silent and expressed genes with the exception of 20 kb immediately upstream of the expressed *Igf2r* promoter. This 20 kb depleted region coincides with four DHS modified by H3K4me2 and H3K9Ac. The results in Figure 3 clearly illustrate that active and repressive modifications show limited spreading and are interspersed in the *Igf2r*/*Air* region.

Figure 2. Parental-Specific Histone Modifications

(A–J) Maternal chromosome.

(A) Map (40 kb) showing maternal expression of *Igf2r* and *Air*. Arrow, *Igf2r* transcription; gray lollipop, silent *Air* transcription start 28 kb downstream of *Igf2r*. Black boxes above line, CpG islands at the *Igf2r* and *Air* promoters. Black bars below line, single-copy regions analyzed by ChIP-PCR. 1–12, primer pairs to assay 11.6 kb of the *Air* promoter region. 13–24, primer pairs to assay 12.7 kb of the *Igf2r* promoter region (Table S4, see note on primer pair 7). Gray boxes with roman numerals, DHS sites. DHSIX is absent from the maternal chromosome, DHSXII is unique to the maternal chromosome.

(B) Typical Input-PCR in MEFB1 cells containing only the maternal *Igf2r* cluster.

(C–E) ChIP-PCR using antibodies against H3K4me3, H3K4me2, and H3K9Ac in MEFB1 cells. For H3K4me3, weak reproducible bands were amplified by primer 7–8 downstream of the *Air* transcription start marked by primer pair 6.

(F–J) ChIP-PCR using antibodies against H3K9me3, H4K20me3, H4K20me1, H3K27me3, and H3K27me1 in MEFB1 cells. One microliter of 1:100 dilution of Input or 1 μl ChIP DNA was amplified per PCR, two to four biological replicas of each ChIP-PCR were performed, and representative images are shown. M, size marker.

(K–T) Paternal chromosome.

(K) Map (40 kb) showing paternal expression of *Igf2r* and *Air*. Details in Figure 2A. Arrow, *Air* transcription; gray lollipop, silent *Igf2r* transcription start 28 kb downstream of *Air*. DHSIX is unique to the paternal chromosome, DHSXII is absent from the paternal chromosome.

(L) Typical Input-PCR in MEFF cells containing only the paternal *Igf2r* cluster. Primer pairs 5 and 6 corresponding to DHSIX generally showed reduced Input signal on the paternal chromosome.

(M–O) ChIP-PCR in MEFF cells using antibodies against H3K4me3, H3K4me2, H3K9Ac.

(P–T) ChIP-PCR in MEFF cells using antibodies against H3K9me3, H4K20me3, H4K20me1, H3K27me3, H3K27me1.

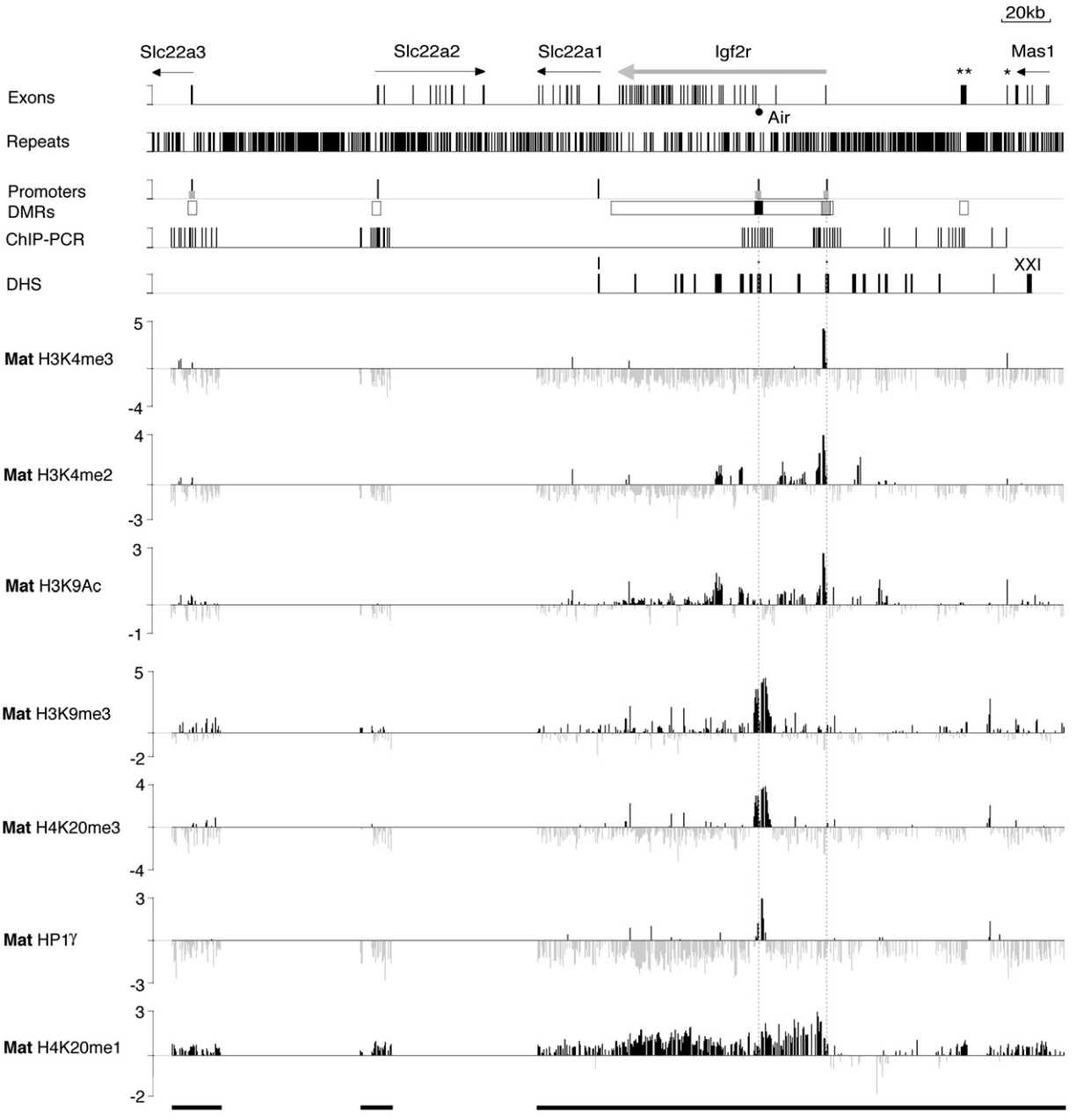

Figure 3. Focal Heterochromatin on the Silent *Air* Promoter

ChIP-Chip profile of active (H3K4me3, H3K4me2, H3K9Ac) and repressive (H3K9me3, H4K20me3, and H4K20me1) histone modifications and the heterochromatin protein HP1γ on the maternal (Mat) *Igf2r* imprinted cluster in MEFB1 cells on the custom PCR tiling array shown in Figure 1B. X axis, 380 kb containing the *Igf2r* imprinted gene cluster that lacked two regions of 58 kb and 61 kb (gaps in the black bars underneath). Exon track, see Figure 1B. Repeats track, bars show total interspersed repeats (simple repeats, MIR, SINE, LINE1, LINE2, LTRs). Promoters track, bars represent transcription start sites (black) and CpG islands (gray). DMRs track, black and gray boxes; respectively, maternal- and paternal-specific DNA methylated regions; white boxes, regions showing no parental differences in DNA methylation (Stoger et al., 1993). ChIP-PCR track, bars represent 61 sites analyzed by PCR around the *Slc22a3*, *Slc22a2*, *Igf2r*, and *Air* promoters and *Au76*-psg. DHS track, bars indicate 21 mapped DHS sites (Pauler et al., 2005). In the seven tracks underneath, each PCR product on the custom tiling array is represented as a single column that is the $\log_2$ signal ratio (ChIP/Input) of the average ratio of medians of eight replicate spots. Vertical dotted lines passing through all tracks mark *Air* and *Igf2r* transcription start sites. Only peaks reproducible in biological replicas (Figure S4) were considered positive.

Figure 4A and Figure S6 show a ChIP-Chip analysis of the same seven modifications on the paternal chromosome on which the *Igf2r* promoter is silenced by the *Air* ncRNA. Active and repressive modifications on the paternal chromosome show the same interspersed, nonspreading patterns as described above for the maternal chromosome. Thus, on the paternal chromosome, H3K4me3 marks are found only on the expressed *Air* promoter and the *L41*-psg, while H3K4me2 and H3K9Ac were found on the expressed *Air* promoter and also on flanking discrete regions. H3K4me2 was also found extensively in *Igf2r* intron 1 that was also marked on the maternal chromosome expressing *Igf2r* (Figure 3). The silent *Igf2r* promoter was modified by a small but reproducible peak of H3K9me3. A peak of H4K20me3 was not detected on the silent *Igf2r* promoter despite positive signals in ChIP-PCR assays in Figure 2Q. This likely reflects different sensitivities of these techniques. HP1γ was also not detected. H4K20me1 showed a widespread distribution with a depletion spanning 20 kb upstream of the expressed *Air* promoter coincident with a region containing DHS modified by H3K4me2 and H3K9Ac.

The paternal chromosome also displayed a broad peak of H3K9me3 and H4K20me3 covering the *Au76*-psg that is contained within the *Air* transcriptional unit but not expressed in MEF cells (Figure S1). This H3K9me3/H4K20me3 peak is not associated with paternal-specific DNA methylation and is found only in differentiated cells and thus is not a germline imprint (Table S3, Figure S7). Figure 4B shows that the paternal-specific H3K9me3 (and H4K20me3, data not shown) signals are lost in cells that contain a 3 kb truncation of the *Air* ncRNA that fails to silence the *Igf2r* promoter (Sleutels et al., 2002).

Of the 21 DHS sites in the profiled region, 11 DHS (VI, VII, VIII, IX, X, XI, XII, XIII, XIV, XV, and XVI) that lie within 20 kb of the expressed *Igf2r* and *Air* promoters showed H3K4me2 modifications (DHS sites are positioned with a resolution of ± 0.5–1.0 kb [Pauler et al., 2005]). In contrast, ten DHS (I, II, III, IV, V, XVII, XVIII, XIX, XX, and XXI) located more than 20 kb away from active promoters lacked H3K4me2 (Figures 3 and 4, Figures S4–S6). Three DHS, VII (6.5 kb upstream to the *Air* promoter), IX (*Air* transcription start), and XII (*Igf2r* transcriptional start), were modified by H3K4me3 + H3K4me2 + H3K9Ac. The remaining modified DHS (VI, VIII, X, XI, XIII, XIV, XV, and XVI) were marked either by H3K4me2 + H3K9Ac or by H3K4me2 and H3K9Ac alone. In two cases, the histone modification appeared to span the region between the neighboring DHS (X + XI spanning 13 kb and XIII+XIV spanning 5.2 kb). Paternal-specific histone modifications were present at DHSIX (*Air* transcription start) and at DHSVII, VIII, XV, and XVI. Maternal-specific histone modifications were found at DHSXII (*Igf2r* transcription start) and at DHSXV and XVI (Table S2).

The Silent *Air* and *Igf2r* Promoter Regions Resemble Heterochromatin

The above Chip-Chip analysis identified three H3K9me3/H4K20me3 peaks; on the silent maternal *Air* promoter, the silent paternal *Igf2r* promoter and the paternal copy of the nonexpressed *Au76*-psg. However, HP1γ was only found on the silent *Air* promoter. Since HP1 is a classic heterochromatin feature, we tested more extensively for the presence of other HP1 isoforms at these regions. Figure S8 shows that the silent maternal *Air* promoter is exclusively marked by HP1α, -β, and -γ. The *Igf2r* promoter lacked HP1α and carried background levels of HP1γ on both silent and active promoters. HP1β, however, exclusively marked the silent *Igf2r* promoter. The paternal copy of the *Au76*-psg lacks specific HP1 binding, demonstrating that H4K20me3 can arise independently of HP1 at this region.

H3K9me3 has been shown to be required for induction of H4K20me3 in pericentric DNA (Schotta et al., 2004). We therefore tested H3K9me3 stability in MEF cells lacking the SUV4-20H methylases. Figure S9 shows that, in these cells, H4K20me3 is reduced, but not lost, over the silent *Air* promoter but is lost over the *Au76*-psg. However, in both cases, H3K9me3 is unaffected. Thus, H3K9me3 modifications are independent of H4K20me3.

To identify which histone methylase mediates H3K9me3 modifications at the silent *Air* and *Igf2r* promoter regions, we performed ChIP-PCR with antibodies to the ESET/SETDB1 H3K9 trimethylase. The silent *Air* promoter showed ESET signals distributed over three primer pairs; ESET signals were weakly present over a similar sized region on the silent *Igf2r* promoter and absent from the *Au76*-psg (Figure 5A). The specificity of the antibody was confirmed by showing absence of a signal on pericentric DNA that carries a SUV39H-dependent H3K9me3 mark (data not shown). To test if the SUV39H methylases contribute to H3K9me3 on *Air*, *Igf2r*, and *Au76*, we examined MEFs lacking these enzymes (Rea et al., 2000). Figures 5B and 5C show that H3K9me3 is retained at the silent *Air* and *Igf2r* promoters and at the *Au76*-psg in cells lacking SUV39H methylases that lack pericentric H3K9me3 (data not shown). Moreover, H3K9me3 plus HP1β and H4K20me3 all increase in SUV39H null cells at the silent *Air* and *Igf2r* promoter. This increase was minimal or absent at the *Au76*-psg.

H3K27me3 Spreads over Large Regions Containing Tissue-Specific Silenced Genes in MEF Cells

The silent *Air* and *Igf2r* genes lack H3K27me3 as determined by ChIP-PCR (Figure 2) and ChIP-Chip (data not shown). However, H3K27me3 (but not H3K9me2 or H3K9me3) was broadly distributed over the promoter regions of the nonexpressed *Slc22a2* and *Slc22a3* genes on both parental chromosomes (Figure 6A). As the custom PCR tiling array lacked complete coverage of the *Slc22a2* and *Slc22a3* genes, we hybridized the same H3K27me3 ChIP/Input samples to a NimbleGen oligonucleotide tiling array. This identified a 300 kb H3K27me3 domain on both the maternal and paternal chromosome that included four genes (*Plg*, *Slc22a3*, *Slc22a2*, and *Slc22a1*) and intergenic regions (Figure 6B). The H3K27me3 domain appeared to have abrupt borders marked by the 5′ end of *Map3k4*

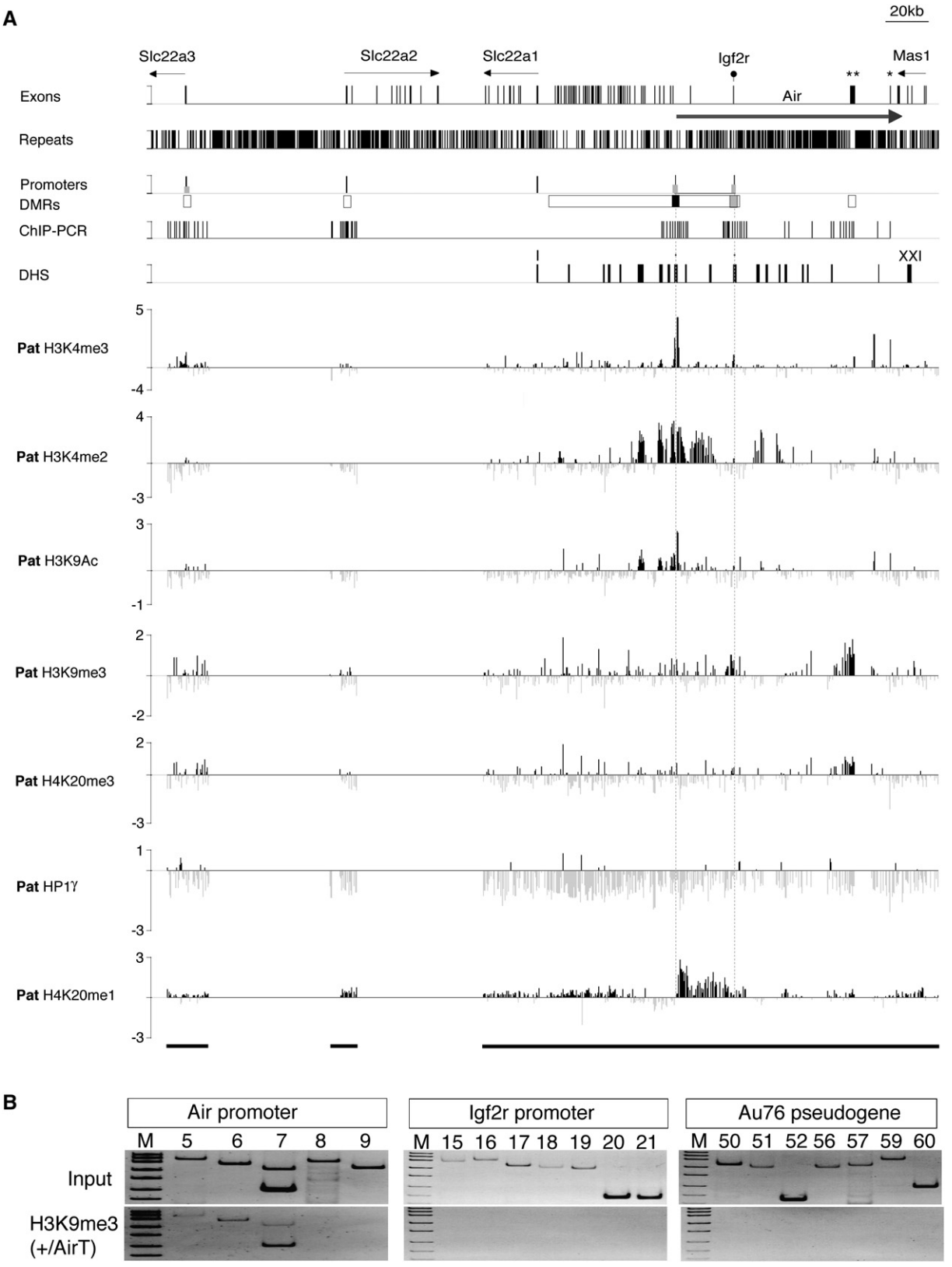
A
20kb
Slc22a3
Slc22a2
Slc22a1
Igf2r
Mas1
Air
Exons
Repeats
Promoters
DMRs
ChIP-PCR
DHS
XXI
Pat H3K4me3
Pat H3K4me2
Pat H3K9Ac
Pat H3K9me3
Pat H4K20me3
Pat HP1γ
Pat H4K20me1
B
Air promoter
Igf2r promoter
Au76 pseudogene
M 5 6 7 8 9
M 15 16 17 18 19 20 21
M 50 51 52 56 57 59 60
Input
H3K9me3
(+/AirT)

and the 3′ end of *Igf2r*. The four genes inside the H3K27me3 domain are repressed in MEF cells, while genes outside this domain are expressed in MEFs (data not shown). Similar H3K27me3 modifications that negatively correlate with gene expression were found on nonimprinted genes lying 43 Mbp distant from *Igf2r* on chromosome 17 (Figure 6C).

DISCUSSION

We have used an imprinted cluster as a model system to examine the type of repressive chromatin associated with silent genes overlapped by antisense transcripts and flanking genes showing tissue-specific silencing. Imprinted genes and a nonexpressed pseudogene overlapped by antisense transcripts were modified by a pattern of focal active chromatin interspersed with focal repressive chromatin that, although resembling pericentric heterochromatin, does not block transcription elongation. However, neighboring groups of tissue-specific silenced genes are contained in a widespread repressed domain devoid of active chromatin marks.

Discrete Foci of Repressive Chromatin Show Limited Spreading

Discrete foci of repressive chromatin were identified on three elements, the silent *Air* promoter, the silent *Igf2r* promoter, and the nonexpressed *Au76*-psg (Table S3). Although the *Air* and *Igf2r* promoters are silenced by different initial events, DNA methylation and *Air* ncRNA expression, respectively (Seidl et al., 2006; Sleutels et al., 2002), both are modified by similar combinatorial marks of H3K9me3, HP1, and H4K20me3, while only H3K9me3 and H4K20me3 modify the nonexpressed *Au76*-psg. As these modifications are typical of heterochromatin at pericentric and telomeric regions and the inactive X chromosome (Chadwick and Willard, 2004; Garcia-Cao et al., 2004; Schotta et al., 2004), we have named them heterochromatin (HC) peaks. Self-propagation or spreading is considered to be a feature of heterochromatin (Grewal and Jia, 2007). In mammals, the model of heterochromatin spreading at centromeres is based on SUV39H methylase inducing H3K9me3 to generate a binding site for HP1 proteins, which then recruit more SUV39H and also SUV4-20H that induces H4K20me3 (Schotta et al., 2004). While on the mammalian inactive X chromosome, the model is based on initial spreading of the *Xist* ncRNA that recruits Polycomb group proteins to induce H3K27me3 and H2A ubiquitylation (Chadwick and Willard, 2004). The HC peaks on the silenced *Air and Igf2r* promoters and *Au76*-psg are, however, limited to 2–6 kb regions and do not spread through the body of the silent gene. Similar short peaks of H3K9me3 are also present upstream of the imprinted *Gtl2* ncRNA, indicating they can occur in other genomic regions (Figure S10). Nonspreading repressive modifications containing H3K9me3 and HP1 limited to a few nucleosomes have also been described for retinoblastoma-mediated and hormone-mediated gene silencing (Ayyanathan et al., 2003; Nielsen et al., 2001). Together, this shows that repressive modifications can be targeted to specific short domains in imprinted and nonimprinted genes by mechanisms that limit spreading.

Similarities between HC Peaks and Pericentric Heterochromatin

Pericentric heterochromatin has been shown to depend on H3K9me3 for subsequent H4K20me3 modification in a pathway suggested to use HP1 to recruit SUV4-20H methylases (Schotta et al., 2004). The H4K20me3 mark in the HC peaks identified here was similarly shown to be dependent on SUV4-20H enzymes. However, HP1 was only associated with HC peaks at *Air* and *Igf2r*, but not at the HC peak on the *Au76*-psg. Thus, H4K20me3 can occur independently of HP1. In addition, reduced H4K20me3 modifications remain on the silent *Air* promoter in the absence of SUV4-20H methylases, indicating the action of other uncharacterized H4K20 trimethylases. It is notable that H3K9me3 was unchanged at HC peaks in SUV4-20H null cells. This indicates that, similar to repressive pathways at pericentric heterochromatin, H3K9me3 modifications occur prior to SUV4-20H induction of H4K20me3.

The initial event at pericentric heterochromatin is SUV39H-mediated induction of H3K9me3. We have shown that HC peaks at the silent *Air* and *Igf2r* promoters, but not that at the *Au76*-psg, bind ESET, an H3K9 trimethylase also known as SETDB1 that is associated with euchromatic regions (Wang et al., 2003). All three HC peaks retain and even intensify H3K9me3 modifications in cells lacking the SUV39H methylases. Thus, ESET is most likely responsible for H3K9me3 at *Air* and *Igf2r* and neither ESET nor SUV39H act on the *Au76*-psg peak. The absence of viable cells lacking ESET (Dodge et al., 2004) and of antibodies suitable for SUV39H ChIP (Table S4) does not allow us to identify ESET as the sole responsible enzyme for H3K9me3 at HC peaks.

Mutually Exclusive Active and Repressed Chromatin States

In MEF cells, the expressed *Igf2r* and *Air* promoters are marked by peaks of H3K4me3 + H3K4me2 + H3K9Ac, while silent promoters lack these modifications. In

Figure 4. Focal Heterochromatin on the Silent *Igf2r* Promoter

(A) ChIP-Chip profile of active and repressive epigenetic marks on the paternal (Pat) *Igf2r* imprinted cluster in MEFF cells. Details as in Figure 3. Only peaks reproducible in biological replicas (Figure S6) were considered positive.

(B) Chip-PCR of the *Air* and *Igf2r* promoters and the *Au76*-psg in cells carrying an *Air* ncRNA truncated from 108 to 3 kb on the paternal allele (Sleutels et al., 2002). This shows a loss of repressive H3K9me3 on *Igf2r* and *Au76*-psg when *Air* is truncated to 3 kb. H4K20me3 was also lost on these two elements (data not shown).

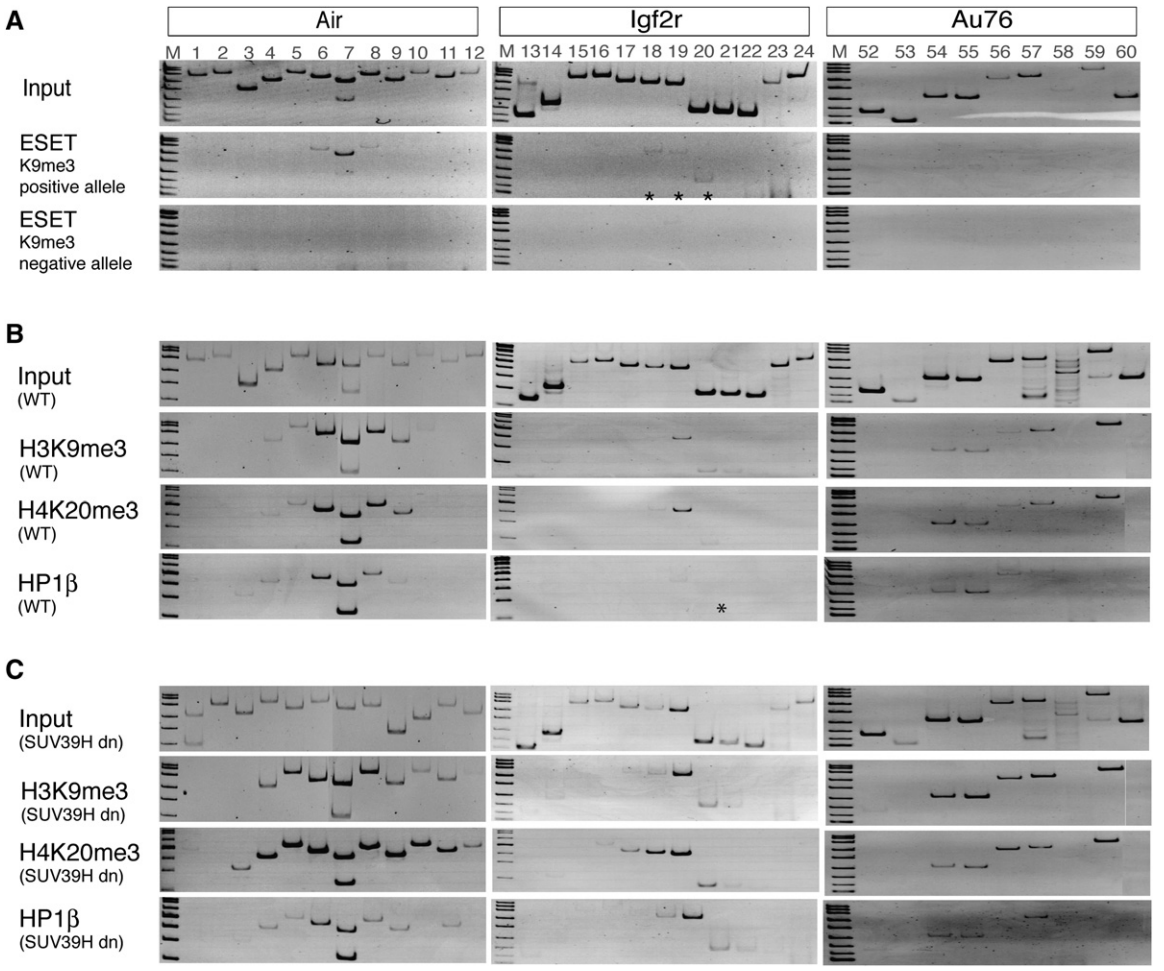

Figure 5. The Histone H3K9 Trimethylase ESET/SETDB1 Binds the *Air* and *Igf2r* HC Peaks

(A) ESET ChIP-PCR at maternal and paternal alleles of the *Air* promoter (left), *Igf2r* promoter (middle), and *Au76*-psg (right), showing that ESET is present at *Air* and *Igf2r* alleles marked by H3K9me3. ESET is absent from *Au76*-psg and pericentric DNA (data not shown) assayed from the same ChIP preparation.

(B and C) (B) ChIP-PCR of the *Air* and *Igf2r* promoters and *Au76*-psg in wild-type control and (C) SUV39H null (SUV39H dn) diploid MEF cells (Peters et al., 2001) using antibodies for H3K9me3, H4K20me3, and HP1β. Increased signals were seen for HC peaks at the *Air* and *Igf2r* promoters, but only minimal changes were seen at *Au76*-psg. SUV39H dn MEFs maintain DNA methylation over the silent *Air* and *Igf2r* promoter regions (data not shown). H3K9me3 is absent from pericentric DNA assayed from the same SUV39H dn ChIP preparation (data not shown) as described (Schotta et al., 2004). *, weak reproducible signals.

contrast, silent promoters were marked by peaks of H3K9me3 + H4K20me3 ± HP1 or by broad domains of H3K27me3, while expressed promoters lack these modifications. Previous analyses identified active and repressive histone modifications on the *Air* and *Igf2r* promoters that were not mutually exclusive but enriched on one parental allele compared to the other (Fournier et al., 2002; Vu et al., 2004). The reason for this difference is not clear but could arise from mixtures of cell types, only some of which express or show imprinted expression of the tested gene (e.g., *Igf2r* in mouse brain is imprinted in glial cells but not in neurons [Yamasaki et al., 2005]). In addition to the *Air* and *Igf2r* promoters, the ChIP-Chip tiling array contains 19 DHS that are present on both parental chromosomes and may be shared by both promoters (Pauler et al., 2005). It is notable that all these DHS lacked specific repressive marks and only DHS within 20 kb of the expressed *Igf2r* and *Air* promoters showed active modifications, either by H3K4me2 + H3K9Ac or by H3K4me2 or H3K9Ac alone (Table S2). We do not yet have an explanation for this pattern of DHS-associated active histone modifications. It is possible that only DHS sites marked by active histone modifications are involved in activation of *Igf2r* and *Air* promoters in MEF cells, but this interpretation needs to be tested further. ChIP-Chip tiling array studies in the human and mouse genome have previously shown that focal active modifications composed of H3K4me1, H3K4me2, and H3 acetylation, but not H3K4me3, mark

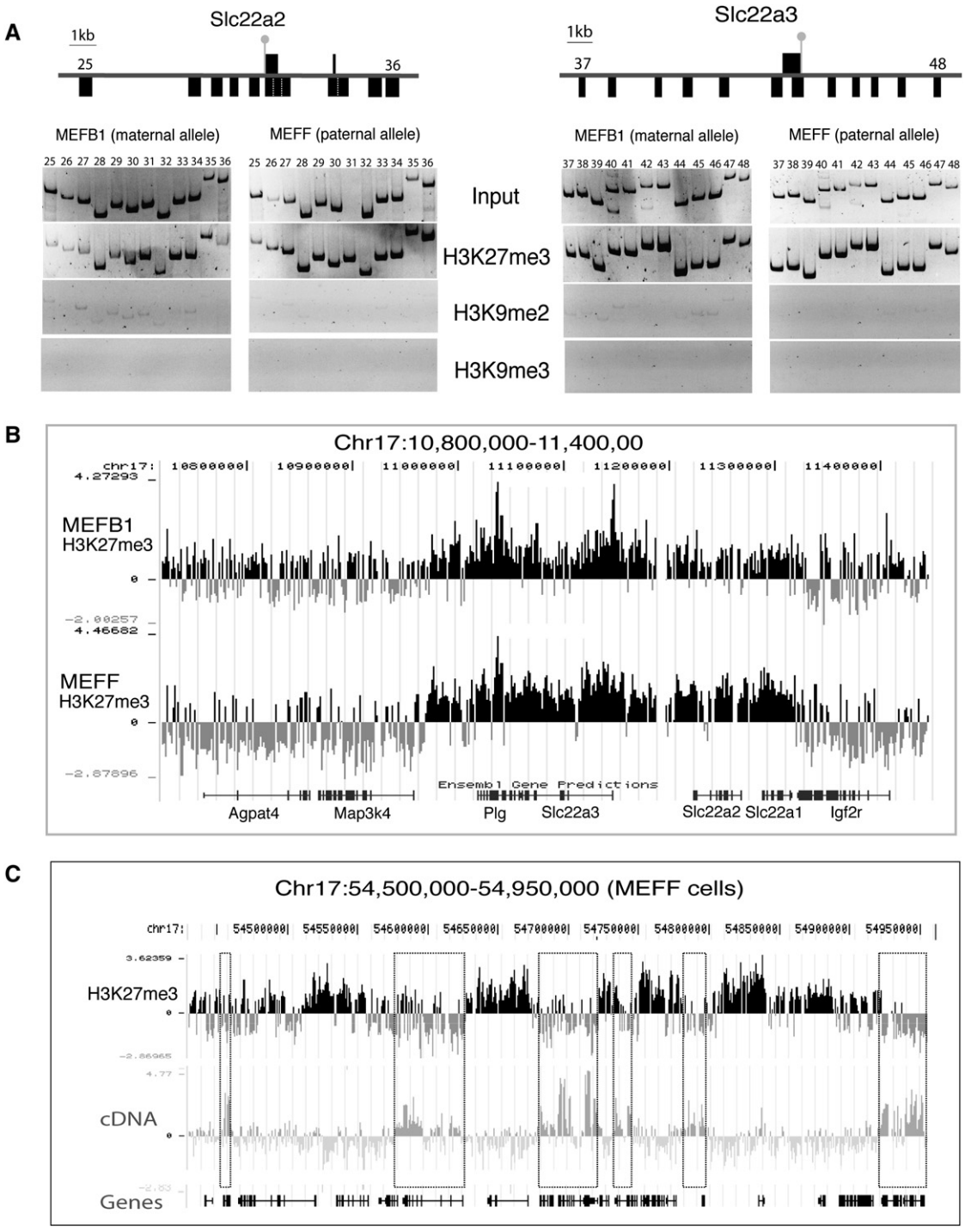

Figure 6. H3K27me3 Modifies Large Domains in MEF Cells

(A) ChIP-PCR showing the distribution of H3K27me3, H3K9me2, and H3K9me3 in a 13 kb and 19 kb region containing the *Slc22a2* (primer pairs 25–36) and *Slc22a3* (primer pairs 37–48) promoters on the maternal and paternal allele in MEFB1 and MEFF cells. Details as in Figure 2A. *Slc22a2* and *Slc22a3* are silent on both parental chromosomes in MEF cells (gray lollipops).

(B and C) NimbleGen mouse chromosome 17 tiling arrays with one 50-mer per 100 bp of single-copy sequence showing the distribution of H3K27me3 over 600 kb containing *Igf2r* on the maternal (MEFB1) and paternal (MEFF) chromosome and a 450 kb region containing nonimprinted genes in MEFF cells. A transcript profile prepared from hybridizing total cell RNA to the tiling array shows that only some of the genes in this 450 kb region are expressed. Expressed genes are marked by dotted boxes that show expression correlates with H3K27me3 depletion. Nonexpressed genes in this region are marked by widespread H3K27me3, which covers the entire transcription unit and intergenic regions. Bars indicate the $\log_2$ signal ratio (ChIP/Input enrichment) of each oligonucleotide on the array. Ensembl genes (http://genome.ucsc.edu) are shown below each array.

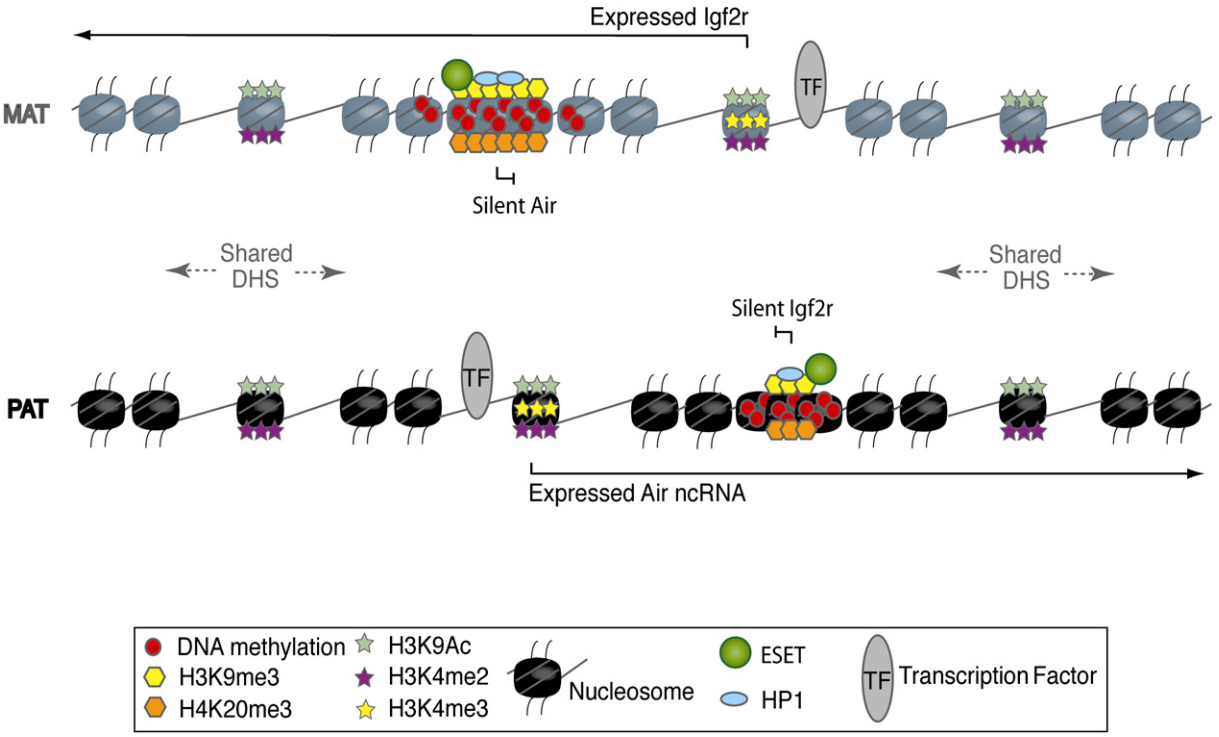

Figure 7. Active and Repressive Chromatin States Intersperse without Overlap

Mutually exclusive active and repressive chromatin modifications that mark the expressed and silent *Air* and *Igf2r* genes that lie 28 kb apart are illustrated for the maternal (MAT) and paternal (PAT) chromosomes. The expressed *Air* and *Igf2r* promoters lack repressive modifications and are marked by H3K4me3, H3K4me2, and H3K9Ac. DHS sites are present on both parental chromosomes, but only those that lie within 20 kb of the expressed promoters are marked by active modifications (H3K4me2 and H3K9Ac, but not by H3K4me3). The silent *Air* and *Igf2r* promoters lack active modifications and are marked by focal HC peaks of H3K9me3, HP1, and H4K20me3 that resemble heterochromatin defined at centromeres, telomeres, and the inactive X chromosome. Note that these HC peaks do not impede transcript elongation from the expressed *Igf2r* and *Air* promoters.

putative regulatory elements of nonimprinted expressed genes (Heintzman et al., 2007; Bernstein et al., 2005). However, these studies did not examine repressive modifications or characterize DHS sites.

Focal Heterochromatin Does Not Block or Impede Transcript Elongation

The ChIP-Chip maps show that the *Air* and *Igf2r* genes contain interspersed peaks of active and repressive chromatin. Notably, the three identified HC peaks in this region lie within actively transcribed gene bodies (Figure 7). On the maternal chromosome, the expressed *Igf2r* transcript runs over the silent *Air* promoter HC peak. On the paternal chromosome, the expressed *Air* transcript runs over HC peaks at the silent *Igf2r* promoter and the nonexpressed *Au76*-psg. The *Air* HC peak does not impede *Igf2r* transcription elongation, as maternal chromosomes carrying the silent modified *Air* promoter or an *Air* promoter deletion express similar levels of *Igf2r* (Wutz et al., 2001). In addition, HC peaks do not arise simply from transcription overlap, as *Air* promoter silencing is independent of *Igf2r* expression (Sleutels et al., 2002, 2003). The *Air* ncRNA has been shown to silence *Igf2r* (Sleutels et al., 2003); here we also show that *Air* ncRNA expression is needed for formation of HC peaks over both the silent *Igf2r* promoter and the *Au76*-psg, reinforcing its specific role as a *cis*-acting silencer. The significance of repressive modifications on the paternal *Au76*-psg allele is not known. It is unlikely to play a role in silencing *Igf2r*, as it is not conserved in the rat genome that shows imprinted *Igf2r* expression (Mills et al., 1998).

Imprinted Gene Silencing and Tissue-Specific Gene Silencing

In contrast to the focal HC peaks found on the imprinted genes in this study, we show that tissue-specific silent genes from two regions on mouse chromosome 17 are marked by a different type of widespread repressive chromatin comprising only H3K27me3. This modification was present on both parental chromosomes, covered the silent gene body and intergenic regions, and was reduced or absent on expressed genes. We also observed that silent genes marked by H3K27me3 lacked H3K9me3 modifications and vice versa. Although our data show that different repressive modifications mark silent imprinted genes and silent tissue-specific genes, we consider it unlikely that imprinted genes carry unique silencing marks. Instead, it is probable that silent nonimprinted genes in

the mammalian genome are modified by the same two types of nonoverlapping repressive chromatin described here, one based on HC peaks and one based on spreading of H3K27me3, that may index permanent or reversible silent states. In support of this argument, large H3K27me3 domains have been identified on silent genes showing cell-type-specific expression in many mouse and human cell types and in large regions of the inactive X chromosome (Bernstein et al., 2006; Chadwick and Willard, 2004; Squazzo et al., 2006). These reports also described a negative correlation between H3K27me3 and H3K9me3.

Models of Epigenetic Gene Silencing in Mammals

We show here (Figure 7) that discrete foci of repressed chromatin resembling classic pericentric heterochromatin can intersperse with focal regions of active chromatin in silent genes overlapped by antisense transcripts. Although we do not yet know the extent of HC peaks in the mammalian genome, the existence of interspersed active and repressive chromatin states questions our current understanding of how chromatin regulates genes in two ways. First, this finding contrasts with the classic view of chromosome chromatin organization in which silent heterochromatin is considered to be restricted to large domains at centromeres, telomeres, and the inactive X chromosome, while active euchromatin is found on chromosome arms that contain the genomes genes (Huisinga et al., 2006). Second, the demonstration that focal heterochromatin exists in the body of actively transcribed genes not only challenges current models of transcription-coupled remodeling processes but also raises questions about the exact role of heterochromatin in gene silencing. Chromosome-wide tiling array maps of repressive chromatin marks will be important tools to resolve these questions.

EXPERIMENTAL PROCEDURES

Chromatin Immunoprecipitation

ChIP was performed as described (Umlauf et al., 2004) with three modifications to minimize nonspecific chromatin binding to protein A Sepharose (PAS): (1) MNase-digested chromatin was precleared with swollen PAS, (2) PAS was pretreated overnight with blocking buffer (10 mM Tris [pH 8.0], 10 mM EDTA [pH 8.0], 1% Triton X-100, 0.01% SDS, 50 mM NaCl, 0.5 mg/ml BSA, 0.25 mg/ml salmon sperm DNA) before binding antigen-antibody complexes, and (3) the PAS-antigen-antibody complex was stringently washed with solutions containing 125, 250, and 500 mM NaCl. Antibodies are listed in Table S4. The resulting ChIP material was analyzed by ChIP-PCR, ChIP-Chip, and/or QPCR. Two to four biological replicas were performed.

Nonquantitative and Quantitative PCR

Nonquantitative PCR was performed with 61 primer pairs (Table S5). PCR mix contained the following: 1 × buffer, 2.5 mM $MgCl_2$, 200 μM dNTPs, 0.5 U Taq polymerase (Promega), and 0.8 M betaine (Sigma). PCR cycles were the following: 94°C/3 min, 30 cycles of 96°C/10 s (12 cycles for pericentric primers), 94°C/30 s, 58°C/1 min, 72°C/1 min, and final extension 72°C/5 min. PCR template was the following: 1 μl of 1:100 diluted Input DNA, 1 μl of ChIP DNA, and 1 μl of mock precipitate. Quantitative real-time PCR assays are listed in Table S1.

Custom PCR Genome Tiling Array Design and Preparation

A custom PCR tiling array spanning 250 kb contained continuous single-copy sequences from bp 12342011–12362277, bp 12420070–12433039, and bp 12493360–12703950 (UCSC Mouse, February 2006, chromosome 17). Repeats were excluded by RepeatMasker (www.repeatmasker.org). PCR products were overlapping with an average size of 430 bp. Control PCR fragments were also spotted on the custom PCR tiling array (Figure S11). PCR reactions were as described above, with the exception of 1.5 M betaine. The PCR template was 2 ng of cosmid (cosOT1, cosMS4, cosMS6, cosMS1, or cos3LA3) or BAC DNA (BACs RP23-84H13, RP23-367L3, or RP23-81B3),or 10 ng of genomic DNA. Products were gel checked, Speedvac concentrated to 10–20 μl, and SSC added to a final 3× concentration. Samples were spotted in eight positions on Nexterion slides (Schott) pretreated with 1-methyl 2-pyrrolidone in blocking solution, with a Promedia Associates Inc. printer (Model PA-MP2000) using SMP3 printing tips (Telechem).

Custom PCR Genome Tiling Array Probe Amplification and Hybridization

ChIP DNA and a 1:100 dilution of Input DNA was amplified using two rounds of a T7 in vitro transcription protocol modified from Liu et al. (2003) (full protocol available upon request) labeled with Alexa 555 or Alexa 647 dyes (Molecular Probes), and ChIP and Input DNA were hybridized together on the tiling array for 18 hr at 42°C. Two biological replicates of MEFB1 and MEFF cells (including a dye swap) were hybridized to the custom PCR tiling array for each mapping experiment. For the high-resolution Oligo tiling arrays, amplified DNA/cDNA was sent for hybridization to NimbleGen Systems or Agilent Technologies Inc.

Custom PCR Genome Tiling Array Scanning and Analysis

Custom PCR tiling array slides were scanned with a GenePix 4000B scanner (Axon Instruments). Microarrays were gridded and the average ratio of medians (with background subtraction) of the eight replicate spots calculated for each PCR product. Individual spots with a ratio greater than or less than two standard deviations from the mean were excluded from the analysis. The average ratio of medians was then $\log_2$ transformed and plotted. Data were displayed with Signal Map (NimbleGen).

Custom PCR Genome Tiling Array Expression Analysis

PolyA+ RNA was isolated from MEFB1 and MEFF cells (Micro Poly[A] Purist, Ambion) and cDNA prepared and labeled and used as described above. The Input sample was as used for ChIP analyses.

Supplemental Data

Supplemental Data include 11 figures, 5 tables, and Supplemental References and can be found with this article online at http://www.molecule.org/cgi/content/full/27/3/353/DC1/.

ACKNOWLEDGMENTS

We thank Robert Feil for the ChIP protocol, Peter Steinlein for tiling array advice, the GEN-AU Epigenetics team for support, and Barlow group members for comments on the manuscript. Project support was from GEN-AU Epigenetic Plasticity of the Mammalian Genome (GZ200.141/1-VI/2006) and the EU-FW6 IP "HEROIC" (LSHG-CT-2005-018883) and NoE "The Epigenome" (LSHG-CT-2004-053433). The authors declare no conflict of interest.

Received: October 20, 2006
Revised: April 12, 2007
Accepted: June 20, 2007
Published: August 2, 2007

REFERENCES

Ayyanathan, K., Lechner, M.S., Bell, P., Maul, G.G., Schultz, D.C., Yamada, Y., Tanaka, K., Torigoe, K., and Rauscher, F.J., 3rd. (2003). Regulated recruitment of HP1 to a euchromatic gene induces mitotically heritable, epigenetic gene silencing: a mammalian cell culture model of gene variegation. Genes Dev. *17*, 1855–1869.

Bernstein, B.E., Kamal, M., Lindblad-Toh, K., Bekiranov, S., Bailey, D.K., Huebert, D.J., McMahon, S., Karlsson, E.K., Kulbokas, E.J., 3rd, Gingeras, T.R., et al. (2005). Genomic maps and comparative analysis of histone modifications in human and mouse. Cell *120*, 169–181.

Bernstein, B.E., Mikkelsen, T.S., Xie, X., Kamal, M., Huebert, D.J., Cuff, J., Fry, B., Meissner, A., Wernig, M., Plath, K., et al. (2006). A bivalent chromatin structure marks key developmental genes in embryonic stem cells. Cell *125*, 315–326.

Chadwick, B.P., and Willard, H.F. (2004). Multiple spatially distinct types of facultative heterochromatin on the human inactive X chromosome. Proc. Natl. Acad. Sci. USA *101*, 17450–17455.

Dodge, J.E., Kang, Y.K., Beppu, H., Lei, H., and Li, E. (2004). Histone H3-K9 methyltransferase ESET is essential for early development. Mol. Cell. Biol. *24*, 2478–2486.

Fournier, C., Goto, Y., Ballestar, E., Delaval, K., Hever, A.M., Esteller, M., and Feil, R. (2002). Allele-specific histone lysine methylation marks regulatory regions at imprinted mouse genes. EMBO J. *21*, 6560–6570.

Garcia-Cao, M., O'Sullivan, R., Peters, A.H., Jenuwein, T., and Blasco, M.A. (2004). Epigenetic regulation of telomere length in mammalian cells by the Suv39h1 and Suv39h2 histone methyltransferases. Nat. Genet. *36*, 94–99.

Grewal, S.I., and Jia, S. (2007). Heterochromatin revisited. Nat. Rev. Genet. *8*, 35–46.

Heintzman, N.D., Stuart, R.K., Hon, G., Fu, Y., Ching, C.W., Hawkins, R.D., Barrera, L.O., Van Calcar, S., Qu, C., Ching, K.A., et al. (2007). Distinct and predictive chromatin signatures of transcriptional promoters and enhancers in the human genome. Nat. Genet *39*, 311–318.

Huisinga, K.L., Brower-Toland, B., and Elgin, S.C. (2006). The contradictory definitions of heterochromatin: transcription and silencing. Chromosoma *115*, 110–122.

Lewis, A., and Reik, W. (2006). How imprinting centres work. Cytogenet. Genome Res. *113*, 81–89.

Liu, C.L., Schreiber, S.L., and Bernstein, B.E. (2003). Development and validation of a T7 based linear amplification for genomic DNA. BMC Genomics *4*, 1–11.

Mancini-Dinardo, D., Steele, S.J., Levorse, J.M., Ingram, R.S., and Tilghman, S.M. (2006). Elongation of the Kcnq1ot1 transcript is required for genomic imprinting of neighboring genes. Genes Dev. *20*, 1268–1282.

Mills, J.J., Falls, J.G., De Souza, A.T., and Jirtle, R.L. (1998). Imprinted M6p/Igf2 receptor is mutated in rat liver tumors. Oncogene *16*, 2797–2802.

Nielsen, S.J., Schneider, R., Bauer, U.M., Bannister, A.J., Morrison, A., O'Carroll, D., Firestein, R., Cleary, M., Jenuwein, T., Herrera, R.E., and Kouzarides, T. (2001). Rb targets histone H3 methylation and HP1 to promoters. Nature *412*, 561–565.

Pauler, F.M., Stricker, S.H., Warczok, K.E., and Barlow, D.P. (2005). Long-range DNase I hypersensitivity mapping reveals the imprinted Igf2r and Air promoters share cis-regulatory elements. Genome Res. *15*, 1379–1387.

Peters, A.H., O'Carroll, D., Scherthan, H., Mechtler, K., Sauer, S., Schofer, C., Weipoltshammer, K., Pagani, M., Lachner, M., Kohlmaier, A., et al. (2001). Loss of the Suv39h histone methyltransferases impairs mammalian heterochromatin and genome stability. Cell *107*, 323–337.

Rea, S., Eisenhaber, F., O'Carroll, D., Strahl, B.D., Sun, Z.W., Schmid, M., Opravil, S., Mechtler, K., Ponting, C.P., Allis, C.D., and Jenuwein, T. (2000). Regulation of chromatin structure by site-specific histone H3 methyltransferases. Nature *406*, 593–599.

Regha, K., Latos, P.A., and Spahn, L. (2006). The imprinted mouse Igf2r/Air cluster—a model maternal imprinting system. Cytogenet. Genome Res. *113*, 165–177.

Schotta, G., Lachner, M., Sarma, K., Ebert, A., Sengupta, R., Reuter, G., Reinberg, D., and Jenuwein, T. (2004). A silencing pathway to induce H3-K9 and H4-K20 trimethylation at constitutive heterochromatin. Genes Dev. *18*, 1251–1262.

Seidl, C.I., Stricker, S.H., and Barlow, D.P. (2006). The imprinted Air ncRNA is an atypical RNAPII transcript that evades splicing and escapes nuclear export. EMBO J. *25*, 3565–3575.

Sleutels, F., Zwart, R., and Barlow, D.P. (2002). The non-coding Air RNA is required for silencing autosomal imprinted genes. Nature *415*, 810–813.

Sleutels, F., Tjon, G., Ludwig, T., and Barlow, D.P. (2003). Imprinted silencing of Slc22a2 and Slc22a3 does not need transcriptional overlap between Igf2r and Air. EMBO J. *22*, 3696–3704.

Solter, D. (2006). Imprinting today: end of the beginning or beginning of the end? Cytogenet. Genome Res. *113*, 12–16.

Squazzo, S.L., O'Geen, H., Komashko, V.M., Krig, S.R., Jin, V.X., Jang, S.W., Margueron, R., Reinberg, D., Green, R., and Farnham, P.J. (2006). Suz12 binds to silenced regions of the genome in a cell-type-specific manner. Genome Res. *16*, 890–900.

Stoger, R., Kubicka, P., Liu, C.G., Kafri, T., Razin, A., Cedar, H., and Barlow, D.P. (1993). Maternal-specific methylation of the imprinted mouse Igf2r locus identifies the expressed locus as carrying the imprinting signal. Cell *73*, 61–71.

Umlauf, D., Goto, Y., Cao, R., Cerqueira, F., Wagschal, A., Zhang, Y., and Feil, R. (2004). Imprinting along the Kcnq1 domain on mouse chromosome 7 involves repressive histone methylation and recruitment of Polycomb group complexes. Nat. Genet. *36*, 1296–1300.

Vu, T.H., Li, T., and Hoffman, A.R. (2004). Promoter-restricted histone code, not the differentially methylated DNA regions or antisense transcripts, marks the imprinting status of IGF2R in human and mouse. Hum. Mol. Genet. *13*, 2233–2245.

Wang, H., An, W., Cao, R., Xia, L., Erdjument-Bromage, H., Chatton, B., Tempst, P., Roeder, R.G., and Zhang, Y. (2003). mAM facilitates conversion by ESET of dimethyl to trimethyl lysine 9 of histone H3 to cause transcriptional repression. Mol. Cell *12*, 475–487.

Wutz, A., Theussl, H.C., Dausman, J., Jaenisch, R., Barlow, D.P., and Wagner, E.F. (2001). Non-imprinted Igf2r expression decreases growth and rescues the Tme mutation in mice. Development *128*, 1881–1887.

Yamasaki, Y., Kayashima, T., Soejima, H., Kinoshita, A., Yoshiura, K., Matsumoto, N., Ohta, T., Urano, T., Masuzaki, H., Ishimaru, T., et al. (2005). Neuron-specific relaxation of Igf2r imprinting is associated with neuron-specific histone modifications and lack of its antisense transcript Air. Hum. Mol. Genet. *14*, 2511–2520.

Zwart, R., Sleutels, F., Wutz, A., Schinkel, A.H., and Barlow, D.P. (2001). Bidirectional action of the Igf2r imprint control element on upstream and downstream imprinted genes. Genes Dev. *15*, 2361–2366.

Accession Numbers

The Gene Expression Omnibus (GEO) accession number for the microarray data reported in this paper is GSE5834.